

Star Cluster Life-times: Dependence on Mass, Radius and Environment

Mark Gieles¹, Henny J. G. L. M. Lamers² and Holger Baumgardt³

¹European Southern Observatory, Casilla 19001, Santiago 19, Chile
email: mgieles@eso.org

²Astronomical Institute, Utrecht University, Princetonplein 5,
3584 CC Utrecht, The Netherlands
email: lamers@astro.uu.nl

³Argelander Institut für Astronomie, Universität Bonn, Auf dem Hügel 71, Bonn, Germany
email: holger@astro.uni-bonn.de

Abstract. The dissolution time (t_{dis}) of clusters in a tidal field does not scale with the “classical” expression for the relaxation time. First, the scaling with N , and hence cluster mass, is shallower due to the finite escape time of stars. Secondly, the cluster half-mass radius is of little importance. This is due to a balance between the relative tidal field strength and internal relaxation, which have an opposite effect on t_{dis} , but of similar magnitude. When external perturbations, such as encounters with giant molecular clouds (GMC) are important, t_{dis} for an individual cluster depends strongly on radius. The mean dissolution time for a population of clusters, however, scales in the same way with mass as for the tidal field, due to the weak dependence of radius on mass. The environmental parameters that determine t_{dis} are the tidal field strength and the density of molecular gas. We compare the empirically derived t_{dis} of clusters in six galaxies to theoretical predictions and argue that encounters with GMCs are the dominant destruction mechanism. Finally, we discuss a number of pitfalls in the derivations of t_{dis} from observations, such as incompleteness, with the cluster system of the SMC as particular example.

Keywords. globular clusters: general, open clusters and associations: general, stellar dynamics, methods: n-body simulations

1. Theoretical predictions of cluster dissolution

1.1. Dynamical evolution in a tidal field

Simulations of star clusters dissolving in a tidal field have shown that the dissolution time ($t_{\text{dis}}^{\text{tid}}$) scales with the relaxation time (t_{rel}) as $t_{\text{dis}}^{\text{tid}} \propto t_{\text{rel}}^{0.75}$ (Baumgardt 2001; Baumgardt & Makino 2003). This non-linear dependence on t_{rel} is due to the finite escape time through one of the Lagrange points (Fukushige & Heggie 2000). The dependence on N , or cluster mass (M_c), can be approximated as $t_{\text{dis}}^{\text{tid}} \propto M_c^{0.62}$, which is accurate for $10^2 \lesssim N \lesssim 10^7$ (Lamers, Gieles & Portegies Zwart 2005). The half-mass radius (r_h) of the cluster does not enter in the results, since it is assumed that clusters are initially “Roche lobe” filling, which implies $M_c \propto r_h^3$, i.e. a constant crossing time.

The assumption of Roche lobe filling clusters is computationally attractive since it avoids having r_h as an extra parameter. However, observations of (young) extra-galactic star clusters show that the dependence of r_h on M_c and galactocentric distance (R_G) is considerably weaker ($r_h \propto M^{0.1} R_G^{0.1}$) than the Roche lobe filling relation ($r_h \propto M^{1/3} R_G^{2/3}$) (Larsen 2004; Scheepmaker, Haas, Gieles *et al.* 2007), implying that massive clusters at large R_G are initially underfilling their Roche lobe.

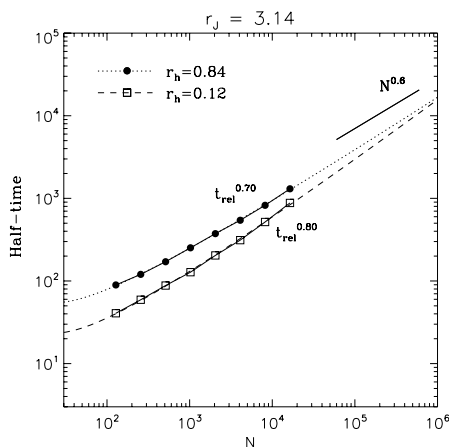


Figure 1. Half-mass time as found from N -body simulations of clusters dissolving in a tidal field. The filled circles represent clusters that initially fill their Roche lobe. The open squares are the results of runs where r_h was seven times smaller.

Gieles & Baumgardt (2007) simulated clusters with varying initial r_h in a tidal field to quantify the importance of r_h . Fig. 1 shows the results of $t_{\text{dis}}^{\text{tid}}$ for two sets of clusters with different initial r_h . The filled circles are for clusters that started tidally limited and the open squares are for runs where the initial r_h was a factor seven smaller. The difference in t_{dis} are within a factor two, while the “classical” expression of t_{rel} predicts a factor $7^{3/2} \simeq 20$. The reason that t_{dis} depends so little on r_h can be understood intuitively: for smaller clusters the tidal field is less important, but the dynamical evolution is faster. These effects happen to balance and result in almost no dependence on r_h . *The crossing of the lines around $N \simeq 10^6$ implies that for globular clusters $t_{\text{dis}}^{\text{tid}}$ is completely independent of r_h .*

This somewhat surprising result means that we can use the r_h independent results for t_{dis} of tidally limited clusters (Baumgardt & Makino 2003) as a general result for $t_{\text{dis}}^{\text{tid}}$ for clusters of different r_h :

$$\frac{t_{\text{dis}}^{\text{tid}}}{\text{Gyr}} = 1.0 \left(\frac{M_c}{10^4 M_\odot} \right)^{0.62} \frac{R_G}{V_G} \frac{220 \text{ km s}^{-1}}{\text{kpc}}. \quad (1.1)$$

From this it follows that a cluster with $M_c = 10^4 M_\odot$ in the solar neighbourhood would dissolve in approximately 8 Gyr due to tidal field. This is much longer than the empirically derived value of 1.3 Gyr (Lamers, Gieles, Bastian, *et al.* 2005), implying that there are additional disruptive effects that shorten the life-time of clusters.

1.2. External perturbations: disruption by giant molecular clouds

It has long been suspected that encounters with giant molecular clouds (GMCs) shorten the life-times of clusters (e.g. van den Bergh & McClure 1980). Gieles, Portegies Zwart, Baumgardt, *et al.* (2006) studied this effect using N -body simulations and found that t_{dis} due to GMC encounters ($t_{\text{dis}}^{\text{GMC}}$) can be expressed in cluster properties and average molecular gas density (ρ_n) as

$$\frac{t_{\text{dis}}^{\text{GMC}}}{\text{Gyr}} = 2.0 \left(\frac{0.03 M_\odot \text{ pc}^{-3}}{\rho_n} \right) \left(\frac{M_c}{10^4 M_\odot} \right) \left(\frac{3.75 \text{ pc}}{r_h} \right)^3. \quad (1.2)$$

Table 1. Columns 1–3: Estimates of tidal field strength, molecular gas densities and resulting predictions for t_4 , the t_{dis} of a cluster with an initial $M_c = 10^4 M_\odot$. Column 4: empirically derived values of t_4 are given, taken from: ¹Gieles *et al.* (2005); ²Lamers, Gieles & Portegies Zwart (2005); ³Lamers, Gieles, Bastian, *et al.* (2005); ⁴Parmentier & de Grijs (2007); ⁵Krienke & Hodge (2004); ⁶Boutloukos & Lamers (2003).

Galaxy	Tidal field R_G/V_G [Myr]	Molecular gas density ρ_n [$10^{-3} M_\odot \text{pc}^{-3}$]	Predicted t_4 [Gyr]	Observed t_4 [Gyr]
M51 ¹	10	450	0.13	0.1
M33 ²	15	25	1.4	0.6
Solar neighbourhood ³	35	30	1.6	1.3
LMC ⁴	30	–	<6.6	>1
NGC6822 ⁵	~35	–	<7.7	~4
SMC ⁶	40	0.5	8.2	8

The scaling of $t_{\text{dis}}^{\text{GMC}}$ with cluster density (M_c/r_h^3) combined with the observed weak dependence of r_h on M_c , $r_h \propto M_c^{0.13}$, results in a similar scaling of the mean $t_{\text{dis}}^{\text{GMC}}$ with M_c as found for $t_{\text{dis}}^{\text{tid}}$, i.e. $\propto M_c^{0.6}$ (1.1).

For the solar neighbourhood ($\rho_n \simeq 0.03 M_\odot \text{pc}^{-3}$) $t_{\text{dis}}^{\text{GMC}} = 2$ Gyr, which combined with the tidal field (1.1) nicely explains the empirically derived t_{dis} of 1.3 Gyr and the observed age distribution of clusters in the solar neighbourhood (Lamers & Gieles 2006).

From (1.1) and (1.2) we see that the predicted t_{dis} scales with the tidal field strength (R_G/V_G) and the inverse of the molecular gas density ($1/\rho_n$). In table 1 we give values for these parameters for six galaxies, combined with predictions for t_4 . The values for ρ_n are taken from Gieles, Portegies Zwart, Baumgardt, *et al.* (2006) (and references therein), Heyer *et al.* (2004); Leroy, Bolatto, Stanimirovic *et al.* (2007) for the solar neighbourhood, M51, M33 and the SMC, respectively. In the next section we compare this to empirically derived values of t_{dis} .

2. Comparison to observations

2.1. Empirically derived t_{dis} values in different galaxies

Under the assumption that t_{dis} scales with M_c , Boutloukos & Lamers (2003) (BL03) introduced an empirical disruption law: $t_{\text{dis}} = t_4 (M_c/10^4 M_\odot)^\gamma$. The value of t_4 and γ can be derived from the age and mass distributions (see BL03 for details). BL03 found a mean γ of $\bar{\gamma} = 0.62$, agreeing nicely with (1.1) and (1.2), and values for t_4 ranging from ~100 Myr to ~8 Gyr. We summarise values of t_4 of clusters in six different galaxies taken from more recent literature in table 1.

Note that R_G/V_G and $1/\rho_n$ roughly increase with increasing t_4 . The variation in R_G/V_G is too small to explain the variation in t_4 , which implies that in the galaxies with short t_4 the disruption is dominated by GMC encounters. *From Table 1 we see that the decreasing trend in the empirical t_4 can be explained by increasing gas density and increasing tidal field strength.*

2.2. The clusters of the SMC

A lot of attention has gone recently to the age distribution (dN/dt) of clusters in the SMC. Rafelski & Zaritsky (2005) (RZ05) found that dN/dt is roughly declining as t^{-1} , which Chandar *et al.* (2006) explain by mass independent cluster disruption† removing

† In fact the authors call their disruption model “infant mortality”, but we prefer to reserve this term for the dissolution of clusters due to gas expulsion. In addition, 3 Gyr old clusters have survived 25% of a Hubble time, so they are not really infant anymore.

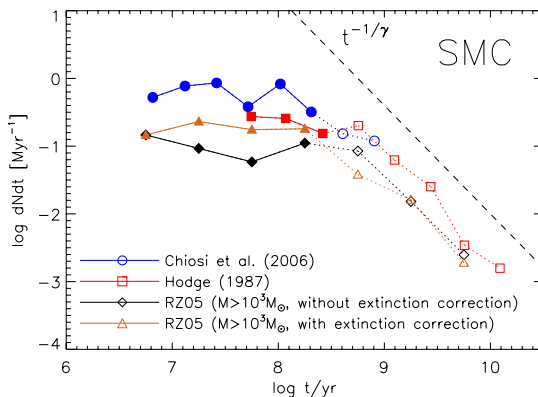


Figure 2. The age distribution (dN/dt) of star clusters in the SMC as found in different studies in literature. The data set of Rafelski & Zaritsky (2005) (RZ05) is very incomplete for low mass clusters at old ages (Gieles, Lamers & Portegies Zwart 2007), so a mass cut at $10^3 M_{\odot}$ was applied. The general trend found in these studies is that dN/dt is flat up to an age of $0.3\text{--}1 \times 10^9$ yr and then it declines as $t^{-1.7}$. The dashed line is the predicted slope for dN/dt at old ages when $t_{\text{dis}} \propto M_c^{\gamma}$, with $\gamma = 0.62$.

90% of the clusters each age dex. Gieles, Lamers & Portegies Zwart (2007) showed that the decline is caused by incompleteness and that the dN/dt is flat in the first ~ 1 Gyr when using a mass limited sample. The dN/dt based on ages which are derived from extinction corrected colours starts declining a bit earlier than the one based on uncorrected colours (Fig. 2). However, the general shape is similar to that found by other authors: a flat part in the first $0.3\text{--}1.0$ Gyr (recently reconfirmed by de Grijs & Goodwin 2007) and then a steep decline ($\propto t^{-1.7}$). When $t_{\text{dis}} \propto M_c^{\gamma}$, then the dN/dt at old ages declines as $t^{-1/\gamma}$ for both mass and magnitude limited samples (BL03). The decline of $t^{-1.7}$ implies $\gamma \simeq 0.6$, in agreement with the theoretical predictions (1.1 and 1.2).

2.3. Selection effects and biases: a cautionary note

Observed cluster samples are always heavily affected by the detection limit, causing the minimum observable cluster mass (M_{min}) to increase with age, due to the fading of clusters. To illustrate this effect we create an artificial cluster population with a constant cluster formation rate (CFR) and with a power-law CIMF with index -2 . In the left panels of Fig. 3 we show the ages and masses (bottom) and the corresponding dN/dt (top) when the sample is mass limited. The dN/dt is flat which is the result of the constant CFR we put it. In the right panel we remove the clusters which are fainter than $M_V = -4.5$. The mass of a cluster at the detection limit, $M_{\text{min}}(t)$, increases with age as $M_{\text{min}}(t) \propto 0.4 M_V^{\text{SSP}}(t)$, where $M_V^{\text{SSP}}(t)$ is the evolution of M_V with age from an SSP model. For a power-law CIMF with index -2 , the resulting dN/dt scales with M_{min} as $dN/dt \propto 1/M_{\text{min}}(t)$ (BL03), which is shown in the top right panel of Fig. 3.

The detection limit is usually expressed in M_V . However, deriving cluster ages from broad band photometry requires the presence of blue filters such as U and B . We show the $M_{\text{min}}(t)$ for a U -band detection limit of $M_U = -5$ as a dashed line in the age vs. mass diagram. The resulting dN/dt (shown as a dashed line in the top right panel) declines approximately as $dN/dt \propto t^{-1.1}$, i.e. steeper than the V -band prediction. *It is of vital importance to understand the effect of incompleteness in different filters before a disruption analyses can be done based on the slope of the dN/dt distribution.*

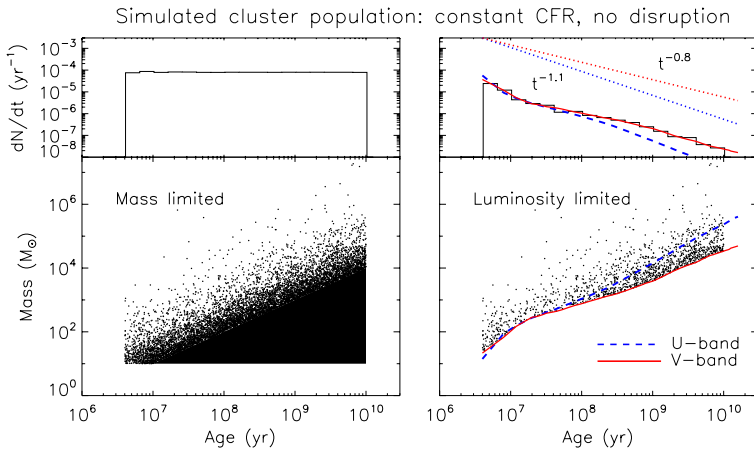


Figure 3. Simulated ages and masses of a cluster population that has formed with a constant cluster formation rate (CFR) and with a power-law CIMF ($N \propto M^{-2}$). In the left panels we show the result of mass limited sample, with $M_{\text{lim}} = 10 M_{\odot}$. In the right panels we assume that the sample is magnitude limited, with $M_{V,\text{lim}} = -4.5$. The limiting mass due to a magnitude limit and the resulting prediction for dN/dt of a magnitude limited sample are shown as full lines (red). The prediction for a U -band limit ($M_U = -5$) is shown as dashed lines (blue). The dotted lines show power-law approximations for the predicted shapes of dN/dt .

References

- Baumgardt, H. 2001, *MNRAS* 325, 1323
 Baumgardt, H. & Makino, J. 2003, *MNRAS* 340, 227
 Boutloukos, S. G. & Lamers, H. J. G. L. M. 2003, *MNRAS* 338, 717
 Chandar, R., Fall, S. M., & Whitmore, B. C. 2006, *ApJ* (Letters) 650, L111
 de Grijs, R. & Goodwin, S. P. 2007, *MNRAS* in press, astro-ph/0709.3781
 Fukushige, T. & Heggie, D. C. 2000, *MNRAS* 318, 753
 Gieles, M., Bastian, N., Lamers, H. J. G. L. M., & Mout, J. N. 2005, *A&A* 441, 949
 Gieles, M. & Baumgardt, H. 2007, *MNRAS* to be submitted
 Gieles, M., Lamers, H. J. G. L. M., & Portegies Zwart, S. F. 2007, *ApJ* 668, 268
 Gieles, M., Portegies Zwart, S. F., Baumgardt, H., Athanassoula, E., Lamers, H. J. G. L. M., Sipior, M., & Leenaarts, J. 2006, *MNRAS* 371, 793
 Heyer, M. H., Corbelli, E., Schneider, S. E., & Young, J. S. 2004, *ApJ* 602, 723
 Krienke, K. & Hodge, P. 2004, *PASP* 116, 497
 Lamers, H. J. G. L. M. & Gieles, M. 2006, *A&A* 455, L17
 Lamers, H. J. G. L. M., Gieles, M., Bastian, N., Baumgardt, H., Kharchenko, N. V., & Portegies Zwart, S. F. 2005, *A&A* 441, 117
 Lamers, H. J. G. L. M., Gieles, M., & Portegies Zwart S. F. 2005, *A&A* 429, 173
 Larsen, S. S. 2004, *A&A* 416, 537
 Leroy, A., Bolatto, A., Stanimirovic, S., Mizuno, N., Israel, F., & Bot C. 2007, *ApJ* 658, 1027
 Rafelski, M. & Zaritsky, D. 2005, *AJ* 129, 2701
 Scheepmaker, R. A., Haas, M. R., Gieles, M., Bastian, N., Larsen, S. S., & Lamers, H. J. G. L. M. 2007, *A&A* 469, 925
 Tanikawa, A. & Fukushige, T. 2005 *PASJ* 57, 155
 van den Bergh, S. & McClure, R. D. 1980, *A&A* 88, 360